SUPPLEMENTARY INFORMATION

Table of Contents **page**

SUPPLEMENTARY TEXT

Additional ImpACT design considerations

To evaluate the ImpACT circuit metal layer thickness (t_m) required for sensing electrical or photonic input, we simulated the response of devices with feasible t_m values ranging between 500 nm and 10 μm. Throughout most of this range, reducing t_m increases the impedance of its inductor component, lowering the device's Q and reducing the coupling efficiency between the ImpACT and the MRI coil. **Supplementary Fig. 2** shows that this has the effect of reducing the change in B_{ImpACT}/B_1 that can be achieved by modulating inputs to the device, lowering its sensitivity. For devices with t_m greater than 8 μm (thicker than twice the skin depth at 400 MHz), performance is approximately constant, with inputs producing up to 63% changes in B_{ImpACT}/B_1. For $t_m < 1$ μm, no discernable change in B_{ImpACT}/B_1 can be produced however.

Although the simulated data of **Fig. 2** and **Supplementary Fig. 2** establish lower bounds of $d = 1$ mm and $t_m = 1$ μm on the fabrication of sensitive ImpACT devices produced with single turn inductors and commercially available compact FETs, we examined additional design factors that could permit improved sensitivity or further miniaturization of the devices in future work. **Supplementary Fig. 3** shows that one route to achieving improved sensitivity is to increase the FET or photoFET's transconductance (g_m), defined as the reciprocal of its drain-source resistance in the fully open state. By increasing g_m fourfold from the value of 5×10^{-3} used in the simulations of **Fig. 2**, the predicted response of a 1 mm ImpACT to a 10 mV input increases by 79%, and the minimum detectable input reaches 11.3 mV or 2.3×10^9 p/s.

A second strategy for improving sensitivity involves increasing the number of turns of the ImpACT inductor coil. **Supplementary Fig. 4** shows that devices with diameters 1 mm, 500 μm, 250 μm, and 100 μm, can achieve 1% changes in B_{ImpACT}/B_1 in response to inputs of 5.6 mV, 5.8 mV, 9.9 mV, and 33 mV respectively.

SUPPLEMENTARY FIGURES

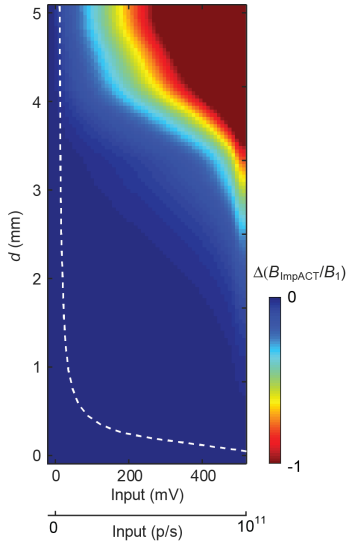

Supplementary Figure 1. Change in enhancement of local RF field intensity as a function of ImpACT dimensions and input strength. MRI effects are modeled as enhancements to the local RF field in the neighborhood of the ImpACT device (B_{ImpACT}/B_1). This graph shows the change in B_{ImpACT}/B_1 at each input amplitude (mV or p/s), with respect to zero input, for each value of the device diameter (d). The white dashed line denotes minimum inputs required to produce 1% change in B_{ImpACT}/B_1, with respect to zero input, for each value of d.

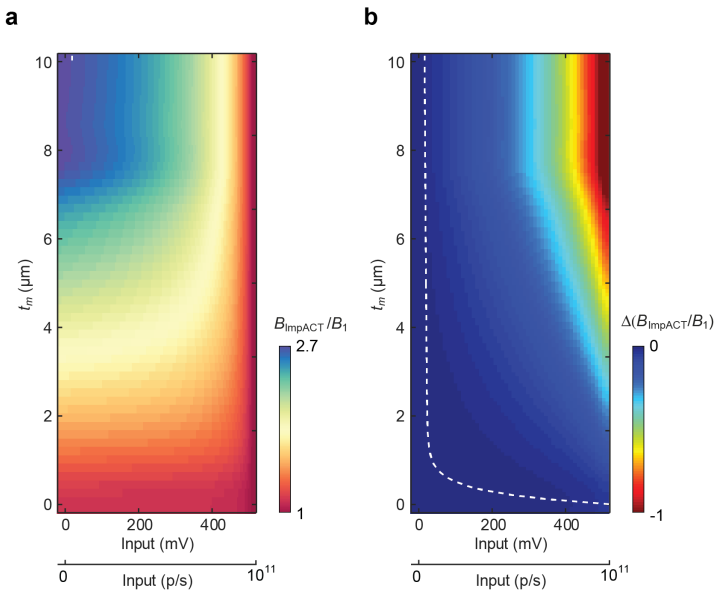

Supplementary Figure 2. Enhancement of local RF intensity as a function of film thickness and input strength. (a) MRI effects are modeled as enhancements to the local RF field in the neighborhood of the device (B_{ImpACT}/B_1), as a function of the ImpACT film thickness (t_m) and the gate input strength in mV or p/s, assuming a device diameter of d = 3 mm. For t_m < 8 μm, the difference between MRI signal in the low *vs.* high input states decreases rapidly, and for t_m < 1 μm falls below the estimated detection limit of 1% change in B_{ImpACT}/B_1 for the entire input range. This sets a lower bound on t_m necessary for constructing effective ImpACT sensors. **(b)** The same results shown as the change in B_{ImpACT}/B_1 at each input amplitude, with respect to zero input, for each value of t_m. The white dashed line denotes minimum inputs required to produce 1% change in B_{ImpACT}/B_1, with respect to zero input, for each value of t_m.

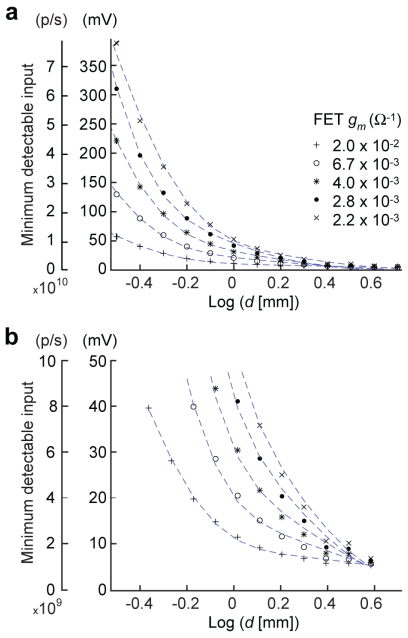

Supplementary Figure 3. ImpACT sensitivity as a function of FET transconductance. Minimum photonic and voltaic input signals predicted to produce 1% change or greater in B_{ImpACT}/B_1 were computed as a function of device diameter (d) for various transconductance (g_m) values shown. Panel **(a)** shows the full range of sensitivities for devices of d = 0.3 to 4 mm; **(b)** depicts the same data, zoomed in to emphasize sensitivities in the 0–50 mV (0–10^{10} p/s) range.

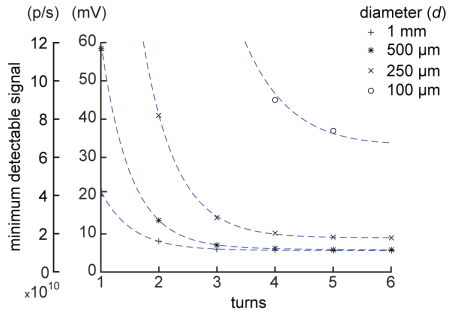

Supplementary Figure 4. Sensitivity of submillimeter multiturn ImpACT devices to voltaic and photonic inputs. Multiturn ImpACTs with diameters 1 mm, 500 µm, 250 µm, and 100 µm, can achieve 1% changes in B_{ImpACT}/B_1 in response to inputs of -5.6 mV, -5.8 mV, -9.9 mV, and -33 mV, respectively.

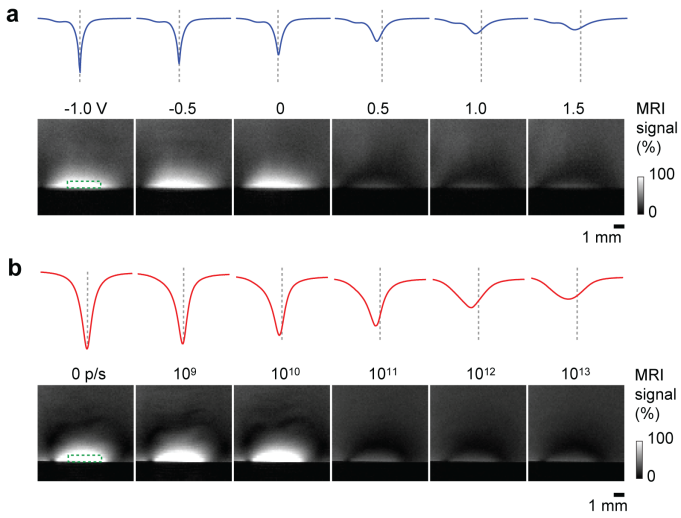

Supplementary Figure 5. Sensitivity of ImpACTs to biologically relevant fields. ImpACTs are initially tuned to resonance frequency of v = 400 MHz, in the absence of input at the FET closed state, and are detuned by input to gate electrode. **(a)** Application of voltage above V_{th} detunes the device and decreases Q (tuning curves at top), causing a reduction of MRI signal (images at bottom). ΔV_{GS} values shown for each condition, and 400 MHz frequency denoted vertical dotted lines with each tuning curve. **(b)** Photonic input from 0–10^{13} p/s into a photoFET-based ImpACT device produces similar responses as the voltage input in panel (a).

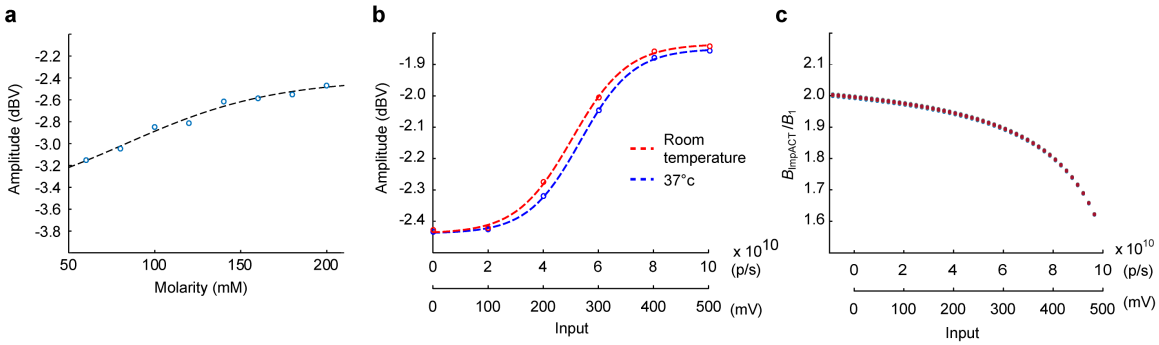

Supplementary Figure 6. ImpACT sensitivity to environmental changes. (a) Experimentally-determined dependence on ionic strength. A 3 mm ImpACT was initially tuned to resonance frequency ν = 400 MHz and juxtaposed to saline solutions of 60-200 mM. Graph shows tuning depth (dBV) at the resonance frequency for different molarity values. **(b)** Temperature-dependence of ImpACT responses to stimulation. Tuning behavior against a 150 mM saline sample was measured across the entire dynamic range of inputs at room temperature (22 °C, red) or 37 °C (blue). **(c)** Simulated ImpACT response profiles predicted for operation at small frequency offsets from the main field resonance frequency (400 MHz). Curves determined over a range of offsets from 399 to 401 MHz are superimposable, showing negligible effect of realistic field distortions of up to 2,500 parts per million.

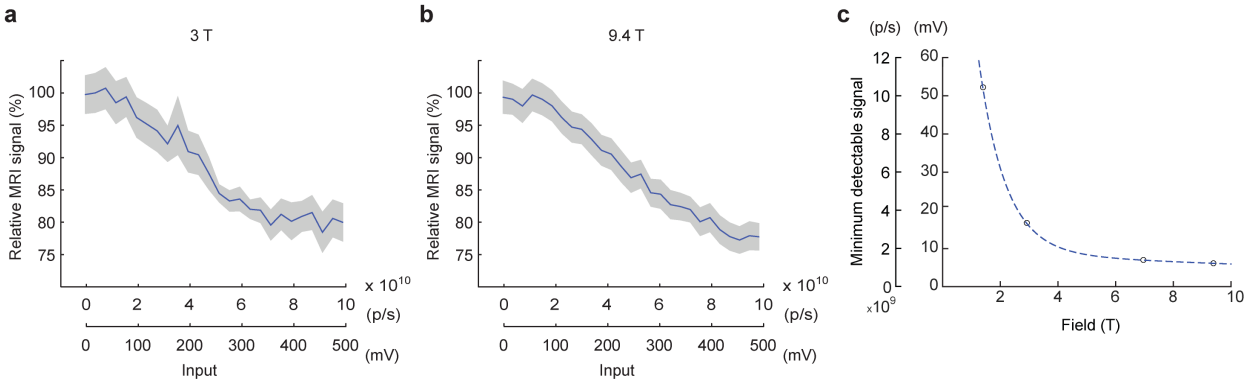

Supplementary Figure 7. ImpACT sensitivity at different MRI field strengths. (a) A 3 mm ImpACT tuned to v = 123.2 MHz was operated in a 3T clinical scanner over the full range of input amplitudes. **(b)** An ImpACT tuned to 400 MHz was similarly operated on a 9.4 T scanner. Shading denotes s.e.m. over 8 voxels in proximity to the ImpACT. **(c)** Simulated sensitivity of ImpACT devices, defined as the input amplitude predicted to produce a 1% change in B_{ImpACT}/B_1, as a function of magnetic field strength.

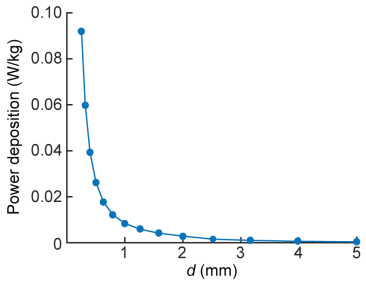

Supplementary Figure 8. Maximum local specific power dissipation by ImpACT devices. For ImpACT devices of different diameters (*d*), we calculated an upper bound on the local specific absorbance rate by computing the maximum specific power deposited in the ImpACT and then assuming that this power is transferred to a spherical volume of tissue of twice the diameter of the device (see Methods for details).

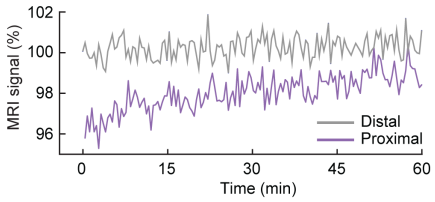

Supplementary Figure 9. Time course of relative MRI signal produced by NanoLuc-expressing cells. The graph shows time courses of NanoLuc-expressing HEK293 cells placed in close juxtaposition to an ImpACT device, following addition of 5 μM furimazine. Signal close to the device (purple) shows relative suppression due to detuning of the device, compared with distal MRI signal (gray), which is not affected by the ImpACT or its tuning status.

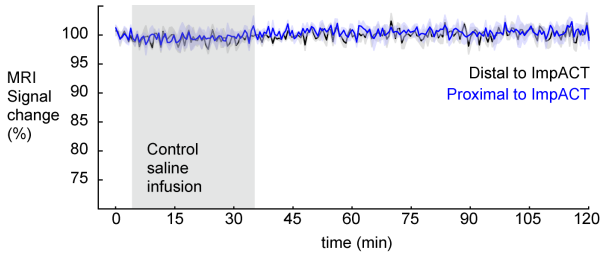

Supplementary Figure 10. MRI monitoring of ImpACT response to sham injections of saline in live rat brains. Control experiments were performed as in Fig. 4g, but with injection of saline solution instead of furimazine. Engineered luciferase (NanoLuc)-expressing HEK-293 cells were grafted into the cerebral cortex and ImpACT device was implanted above the cells. An infusion cannula was inserted nearby for infusion of saline. Saline infusion (t = 5-35 mins) resulted in no significant signal enhancement in the center of the ImpACT device (paired t-test p = 0.9309) which remained tuned throughout the experiments. Mean time course depicts relative MRI signal proximal (blue) and distal (black) to the ImpACT (shaded margins denote s.e.m. over three animals). Saline infusion period indicated by gray box. Signal change axis spans 70-100 % as in Fig. 4g.

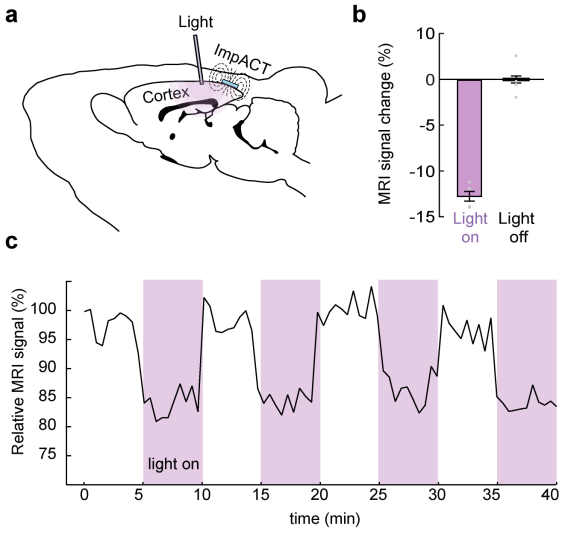

Supplementary Figure 11. Reversible detuning of an ImpACT device in live rat brain. **(a)** A 3 mm photosensitive ImpACT device was implanted above the cortical surface of an anesthetized rat and an optical fiber was inserted 1 mm anterior to implantation site for light-dependent modulation. **(b)** Application of 5 x 10^{10} p/s generated MRI signal decrease of 12.7 ± 0.7 % in cortical region proximal to the device. Bars denote mean values, error bars denote s.e.m. (n = 4); individual data measurements indicated by gray dots. **(c)** Relative MRI signal proximal to ImpACT device in response to intermittent application of 5 x 10^{10} p/s through the optical fiber. Purple shaded areas denote 5 min epochs of light application.